

See discussions, stats, and author profiles for this publication at: <https://www.researchgate.net/publication/263939694>

# Tuning Fluorinated Benzotriazole Polymers through Alkylthio Substitution and Selenophene Incorporation for Bulk Heterojunction Solar Cells

ARTICLE in MACROMOLECULES · MARCH 2014

Impact Factor: 5.8 · DOI: 10.1021/ma5001095

---

CITATIONS

21

---

READS

37

## 4 AUTHORS, INCLUDING:



Liang Yan

University of North Carolina at Chapel Hill

31 PUBLICATIONS 379 CITATIONS

[SEE PROFILE](#)



Wentao Li

University of North Carolina at Chapel Hill

10 PUBLICATIONS 363 CITATIONS

[SEE PROFILE](#)



Wei You

University of North Carolina at Chapel Hill

81 PUBLICATIONS 4,355 CITATIONS

[SEE PROFILE](#)

## Tuning Fluorinated Benzotriazole Polymers through Alkylthio Substitution and Selenophene Incorporation for Bulk Heterojunction Solar Cells

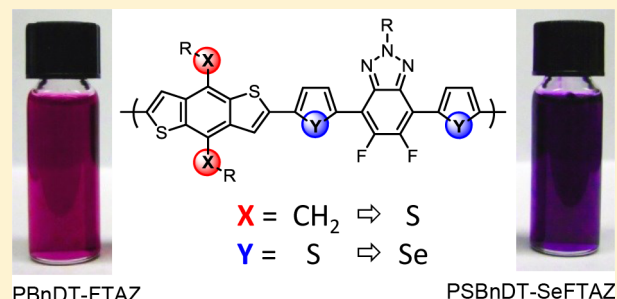
Rycel L. Uy,<sup>†</sup> Liang Yan,<sup>†</sup> Wentao Li,<sup>†</sup> and Wei You\*,<sup>†,‡</sup>

<sup>†</sup>Department of Chemistry, University of North Carolina at Chapel Hill, Chapel Hill, North Carolina 27599-3290, United States

<sup>‡</sup>State Key Laboratory of Advanced Technology for Materials Synthesis and Processing, Wuhan University of Technology, Wuhan 430070, P. R. China

### S Supporting Information

**ABSTRACT:** As a high-performing, medium band gap donor polymer achieving over 7% in bulk heterojunction (BHJ) solar cells with a thick active layer, PBnDT-FTAZ has demonstrated unique photovoltaic properties that have not yet been fine-tuned. In this study, three new polymers (PSBnDT-FTAZ, PBnDT-SeFTAZ, and PSBnDT-SeFTAZ) are designed to determine how the FTAZ system would respond to further structural modifications. Specifically, we aimed to answer (a) whether alkylthio substitution could increase the open circuit voltage ( $V_{oc}$ ) of the related BHJ device and (b) whether selenophene incorporation could decrease the band gap of the FTAZ polymer and lead to an improved short circuit current ( $J_{sc}$ ), while PBnDT-FTAZ's other desirable attributes (high fill factor and thick active layer) could still be retained. We found that although the  $V_{oc}$  of the alkylthio-substituted polymers (PSBnDT-FTAZ and PSBnDT-SeFTAZ) did not appreciably increase, selenophene-incorporated polymers (PBnDT-SeFTAZ and PSBnDT-SeFTAZ) indeed showed lowered band gaps of 1.7 eV. In particular, the smaller band gap of PBnDT-SeFTAZ led to a larger  $J_{sc}$  in its BHJ solar cells than that of the original PBnDT-FTAZ solar cells. Each polymer reached moderate efficiencies (1.87–5.72%) while retaining a thick active layer (~300 nm), demonstrating the further potential of the FTAZ system for organic photovoltaics.



### INTRODUCTION

The discovery of new high-performing donor polymers for single junction organic solar cells has begun to taper off,<sup>1</sup> and efforts have shifted toward new device architectures in order to advance the device efficiencies.<sup>2,3</sup> Nevertheless, as the critical component to organic solar cells, donor polymers still remain one of the key determinants of power conversion efficiency. Therefore, further research on the design and synthesis is well justified. While *de novo* designs of conjugated materials—guided by further understanding of the operating mechanism of organic solar cells<sup>4–6</sup>—would arguably be the best strategy to dramatically improve the efficiency, further optimization of existing high-performing polymers by fine-tuning their molecular structure remains an effective approach to improve device performance. Fortunately, such optimization/fine-tuning of molecular structures does not have to be polymer-specific. In fact, of the top performing polymers achieving over 7% efficiency in their bulk heterojunction (BHJ) photovoltaic devices, many are similar in structure—containing mostly thiophene-based moieties and utilizing the donor–acceptor approach.<sup>7–20</sup> These structural similarities offer great opportunities to translate several simple but effective strategies from one polymer system to another, with the goal of achieving higher device efficiency.

We recently reported a high-performing polymer for BHJ solar cells, PBnDT-FTAZ,<sup>9</sup> a “weak donor–strong acceptor” copolymer<sup>17</sup> that consists of alternating units of benzodithiophene (BnDT) and fluorinated benzotriazole (FTAZ). This polymer has attracted a lot of attention due to several unique properties. For example, with a band gap of 2.0 eV, PBnDT-FTAZ can still achieve over 7% efficiency in its BHJ devices with PC<sub>61</sub>BM (phenyl-C<sub>61</sub>-butyric acid methyl ester). With a respectable open circuit voltage ( $V_{oc}$ ) of 0.8 V, PBnDT-FTAZ can serve as the medium band gap polymer that is required in tandem solar cells. Furthermore, PBnDT-FTAZ devices also exhibit a noticeably high fill factor (FF) of over 70%, which is indicative of significantly reduced charge recombination. Most polymers that have reached similar efficiencies only demonstrate fill factors in the range of 50–60%. In addition, PBnDT-FTAZ solar cells still achieve over 6% efficiency at a nearly 1000 nm thick active layer while most other high-performing polymers can only do so at thin films of 100–200 nm.<sup>1,9,18</sup> Finally, our recent study of PBnDT-FTAZ devices reported high efficiencies independent of the active layer’s morphology.

Received: January 14, 2014

Revised: March 16, 2014

Published: March 31, 2014

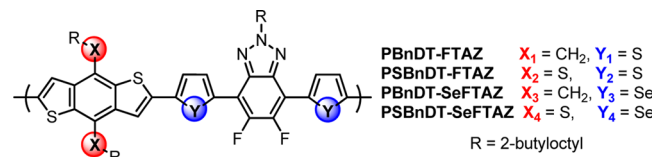
and thickness due to this polymer's lower miscibility with PC<sub>61</sub>BM.<sup>19</sup>

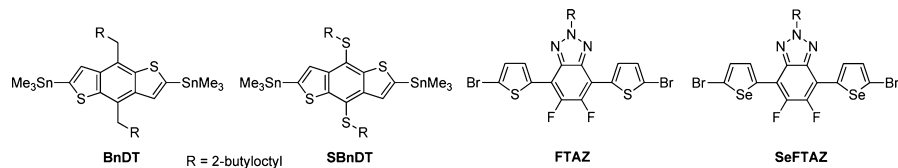
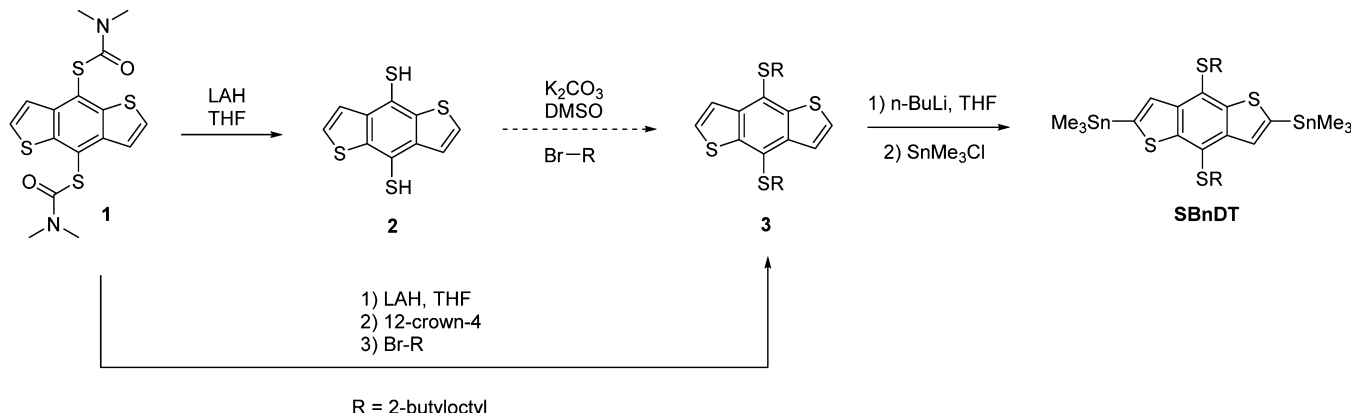
Nevertheless, there is still room to potentially improve PBnDT-FTAZ's photovoltaic performance via fine-tuning its chemical structure. For example, PBnDT-FTAZ's large band gap of ~2.0 eV limits the highest short circuit current ( $J_{sc}$ ) its BHJ device can reach. In addition, devices based on PBnDT-FTAZ only show a moderate  $V_{oc}$  of 0.8 V.<sup>9</sup> Increasing this system's  $J_{sc}$  by narrowing the band gap of PBnDT-FTAZ and enhancing its  $V_{oc}$  via structural modifications while still maintaining its high fill factor would strategically increase the overall efficiency.

Recently, two structural modifications of donor polymers have emerged demonstrating success in (1) improving the  $V_{oc}$  of related BHJ devices and (2) decreasing the band gap of modified polymers. Lee et al. published a series of benzodithiophene (BnDT) homopolymers exhibiting a very high  $V_{oc}$  of 0.99 V in their BHJ devices when alkylthio chains were substituted in place of alkoxy chains on the BnDT unit. The authors attributed the higher  $V_{oc}$  to the sulfur atom lowering the HOMO level of the BnDT homopolymer and the S–S interactions facilitating better  $\pi$ – $\pi$  stacking.<sup>20–22</sup> This interesting discovery inspired us to incorporate a similar strategy into our structural optimization of PBnDT-FTAZ. During preparation of this manuscript, Li and co-workers<sup>23</sup> reported high  $V_{oc}$  values for BHJ devices based on alternating copolymers of dialkylthio-substituted benzodithiophene and monofluorinated benzotriazole with either flanking thiophenes (0.88 V) or furans (0.91 V). These new results further indicate that such alkylthio substitutions could also enhance the  $V_{oc}$  of our FTAZ system.

To decrease a polymer's band gap, modifying the heteroatoms has long been a common strategy.<sup>24,25</sup> Rather than using thiophene or furan, we were interested in incorporating selenophene, a strategy that has been demonstrated by several studies to decrease the band gap of benzothiadiazole<sup>26–31</sup> and diketopyrrolopyrrole<sup>32–35</sup> based polymers as well as the band gap of other semiconducting materials.<sup>36–38</sup> This has also been illustrated in studies comparing polyselenophene vs polythiophene, which have shown that Se-based compounds are more polarizable and exhibit better charge mobility.<sup>36,39</sup> In one particular example, Dou et al. found that going from furan to thiophene to selenophene led to a systematic decrease in the band gap of their diketopyrrolopyrrole-based polymers.<sup>32</sup> Because of selenophene's lower resonance stabilization energy, selenophene-based polymers easily dearomatize into their quinoid form, causing more double-bond character between units, thereby decreasing the band gap and increasing light absorption.<sup>28,39</sup> Chen et al. also discovered that the band gap of selenophene-based polymers decreased because the LUMO was predominantly lowered while the HOMO was relatively unchanged. Density functional theory (DFT) calculations of these polymers showed that the LUMO tends to exist on the selenophene moieties while the HOMO does not.<sup>28</sup> Such a feature would be especially beneficial for PBnDT-FTAZ in order to decrease the polymer's band gap by lowering its LUMO level while still maintaining its ideal HOMO level of ~5.4 eV.<sup>9,40,41</sup>

Herein, we report the results of adopting the two aforementioned strategies to modify our original PBnDT-FTAZ polymer. Specifically, three FTAZ polymer derivatives (Figure 1) were synthesized after substituting alkylthio chains



**Chart 1. Candidate Monomers for FTAZ Polymer Derivatives****Scheme 1. One-Pot Modification to SBnDT Synthesis****Table 1. Polymerization Results for FTAZ Polymers**

	$M_n$ [kg/mol]	$M_w$ [kg/mol]	PDI	yield [%]
PBnDT-FTAZ	61	134	2.20	96
PSBnDT-FTAZ	41	131	3.17	94
PBnDT-SeFTAZ	38	113	3.00	91
PSBnDT-SeFTAZ	39	187	4.75	92

<sup>a</sup>GPC measurements were taken in 1,2,4-trichlorobenzene at 135 °C; the molecular weight was approximated relative to the polystyrene standards.

**Table 2. Optical and Electrochemical Properties of FTAZ Polymers**

	UV-vis absorption				cyclic voltammetry	
	CHCl <sub>3</sub> solution		film		$E_{\text{ox.onset}}$ (V)	$E_{\text{red.onset}}$ (V)
	$\lambda_{\text{max}}$ [nm]	$E_g$ [eV]	$\lambda_{\text{max}}$ [nm]	$E_g$ [eV]	HOMO [eV]	LUMO [eV]
PBnDT-FTAZ	575	1.92	577	1.91	-5.40	-3.10
PSBnDT-FTAZ	572	1.96	542	1.85	-5.30	-3.00
PBnDT-SeFTAZ	607	1.81	611	1.79	-5.42	-3.55
PSBnDT-SeFTAZ	598	1.78	608	1.78	-5.50	-3.40

with their thiophene counterparts (PBnDT-FTAZ and PSBnDT-FTAZ). Although alkylthio substitutions typically lower the HOMO level,<sup>28,21</sup> both the HOMO and LUMO levels are slightly increased for PSBnDT-FTAZ. The thiophene moiety of FTAZ is perhaps better able to delocalize both the HOMO and LUMO levels as opposed to the selenophene moiety of SeFTAZ.<sup>28</sup> Overall, the HOMO levels of the selenophene polymers changed slightly while their LUMO levels were lowered much more. This demonstrates that incorporating selenophene into FTAZ polymers can successfully tune the LUMO levels of this polymer system as it did for others previously reported.

## PHOTOVOLTAIC PROPERTIES

The bulk heterojunction solar cell devices of the four FTAZ polymers blended with PC<sub>61</sub>BM in 1:2 weight ratio achieved efficiencies of 1.87–6.81% as shown in Table 3 and Figure 3. We implemented rather thick films of roughly the same thicknesses (~300 nm) for all devices in order to probe how these structural modifications (alkylthio substitution and selenophene incorporation) would impact the previously obtained high  $J_{\text{sc}}$  and FF with a rather thick active layer of the original PBnDT-FTAZ polymer.<sup>9</sup> Indeed, we were able to

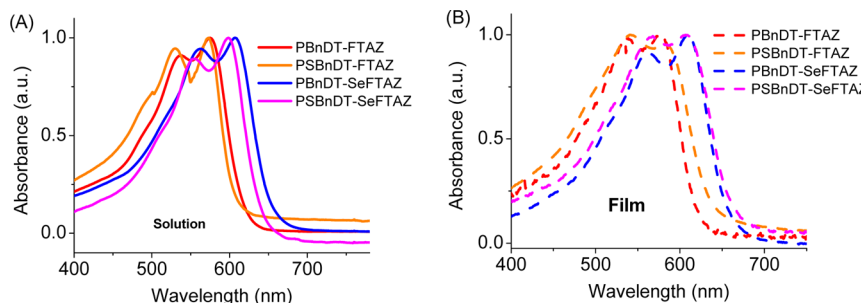
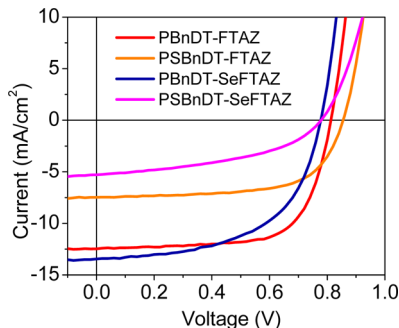
**Figure 2. UV-vis absorption spectra of FTAZ polymers (A) in solution and (B) as film.**

Table 3. Photovoltaic Performance of FTAZ Polymers Based Solar Cells

polymer	thickness [nm]	$J_{sc}$ [mA/cm <sup>2</sup> ]	$V_{oc}$ [V]	FF [%]	PCE [%]
PBnDT-FTAZ	327	12.60 ± 0.53	0.813 ± 0.002	66.5 ± 1.4	6.81 ± 0.26
PSBnDT-FTAZ	317	7.46 ± 0.35	0.850 ± 0.002	63.8 ± 1.0	4.06 ± 0.22
PBnDT-SeFTAZ	311	13.44 ± 0.45	0.779 ± 0.002	54.6 ± 1.3	5.72 ± 0.24
PSBnDT-SeFTAZ	336	5.23 ± 0.32	0.782 ± 0.003	45.9 ± 1.9	1.87 ± 0.11

Figure 3. Characteristic  $J$ - $V$  curves of solar cell with FTAZ polymers under 100 mW/cm<sup>2</sup> AM 1.5G illumination.

reproduce the device characteristics of the original PBnDT-FTAZ with this new batch (Figure 3 and Table 3), which serves as the benchmark to comparatively evaluate the device performance of the three new FTAZ polymer derivatives.

**Impact of Alkylthio Substitution.** BHJ solar cells based on the alkylthio-substituted polymers (PSBnDT-FTAZ and PSBnDT-SeFTAZ) showed a minor increase in  $V_{oc}$  when compared with their alkyl chain analogues (PBnDT-FTAZ and PBnDT-SeFTAZ) (Table 3). However, the  $J_{sc}$  values were significantly lowered, mainly due to a large drop in external

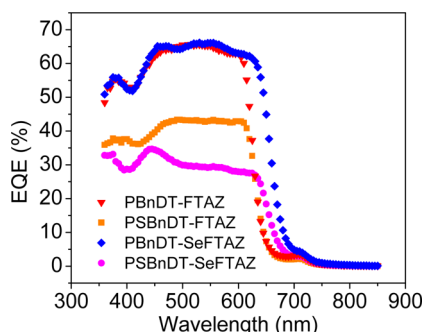


Figure 4. External quantum efficiency (EQE) data of FTAZ-based BHJ solar cells.

quantum efficiency (EQE) as shown in Figure 4. We cite two possible causes for the observed low  $J_{sc}$  and EQE: First, the hole mobilities of all four FTAZ polymers, measured via the space charge limited current (SCLC) method, indicate that the alkylthio-substituted polymers have much lower hole mobilities

Table 4. Hole Mobility of FTAZ Polymers and the Measured Surface Roughness for Their BHJ Blends with PC<sub>61</sub>BM

	$\mu_{hole}$ [cm <sup>2</sup> /(V s)]	roughness [nm]
PBnDT-FTAZ	$1.19 \times 10^{-3}$	1.7
PSBnDT-FTAZ	$2.90 \times 10^{-4}$	7.6
PBnDT-SeFTAZ	$3.46 \times 10^{-4}$	5.5
PSBnDT-SeFTAZ	$1.72 \times 10^{-4}$	3.4

than those of their alkyl-substituted counterparts (Table 4). The low hole mobilities of PSBnDT-FTAZ and PSBnDT-SeFTAZ cannot sustain the hole transport across such thick films (>300 nm) without being significantly impacted by charge recombination losses. Second, atomic force microscopy (AFM) of the morphology of these four films (Figure 5) clearly indicates that the surface roughness of the three new FTAZ polymers is much larger than that of the original PBnDT-FTAZ. The increased surface roughness implies large phase aggregations in the active layers of these new FTAZ devices are possibly due to nonoptimal processing conditions. In fact, the rough morphology of the selenophene-based polymers was anticipated, as these two polymers (SeFTAZ) were less soluble in the processing solvents. Polymers of lower solubility usually lead to less favorable morphologies when blended with fullerenes as previous studies have documented.<sup>36,39,42</sup> In short, the nonideal morphologies, coupled with the relatively low hole mobilities of two alkylthio-substituted polymers, likely resulted in the lowered  $J_{sc}$  values of the PSBnDT-FTAZ- and PSBnDT-SeFTAZ-based devices.

**Impact of Selenophene Incorporation.** For the two polymers based on BnDT, the PBnDT-SeFTAZ-based device showed a higher  $J_{sc}$  than that of the PBnDT-FTAZ control. This very encouraging result can be attributed to (a) the increased light absorption of PBnDT-SeFTAZ due to its smaller band gap (Figure 2 and Table 2) and (b) its relatively high hole mobility among the three new FTAZ derivatives (Table 4). However, the nonideal morphology of PBnDT-SeFTAZ's active layer caused a noticeable drop in the FF from 66.5% to 54.6% and prevented the efficiency from surpassing PBnDT-FTAZ (Table 3 and Figure 3). For the two polymers based on SBnDT, PSBnDT-SeFTAZ showed a lower HOMO level than its thiophene counterpart PSBnDT-FTAZ ( $-5.50$  vs  $-5.30$  eV) and a lower surface roughness (3.4 vs 7.6 nm), but PSBnDT-SeFTAZ exhibited a lower  $V_{oc}$  (0.782 vs 0.850 V) in its BHJ devices. It is likely that the photovoltaic properties of SeFTAZ-based materials are not as insensitive to morphology changes as FTAZ polymers have demonstrated.<sup>19</sup> Ultimately, the expected synergistic effect of higher  $V_{oc}$  and  $J_{sc}$  for PSBnDT-SeFTAZ was mostly mitigated by the lowering  $J_{sc}$  effect of the alkylthio-substituted benzodithiophene (SBnDT) unit.

**Impact of 1,8-Diodooctane (DIO) Additive.** For their devices based on the alternating copolymers of dialkylthio-substituted benzodithiophene and monofluorinated benzotriazole, Li and co-workers observed significant improvements in both current (over 30% increase) and fill factor (from 57% to 71%) after applying DIO as the processing additive.<sup>23</sup> Since PBnDT-SeFTAZ-based devices exhibited the most favorable properties of the new polymer solar cells, a similar approach was attempted using a 3% DIO additive for further optimization of film morphology. Unfortunately, no increase in photovoltaic performance was observed (Table S1). Please note that using an additive to improve the efficiency does not ensure success for every polymer-based OPV device. In addition, there are many other strategies (such as surface

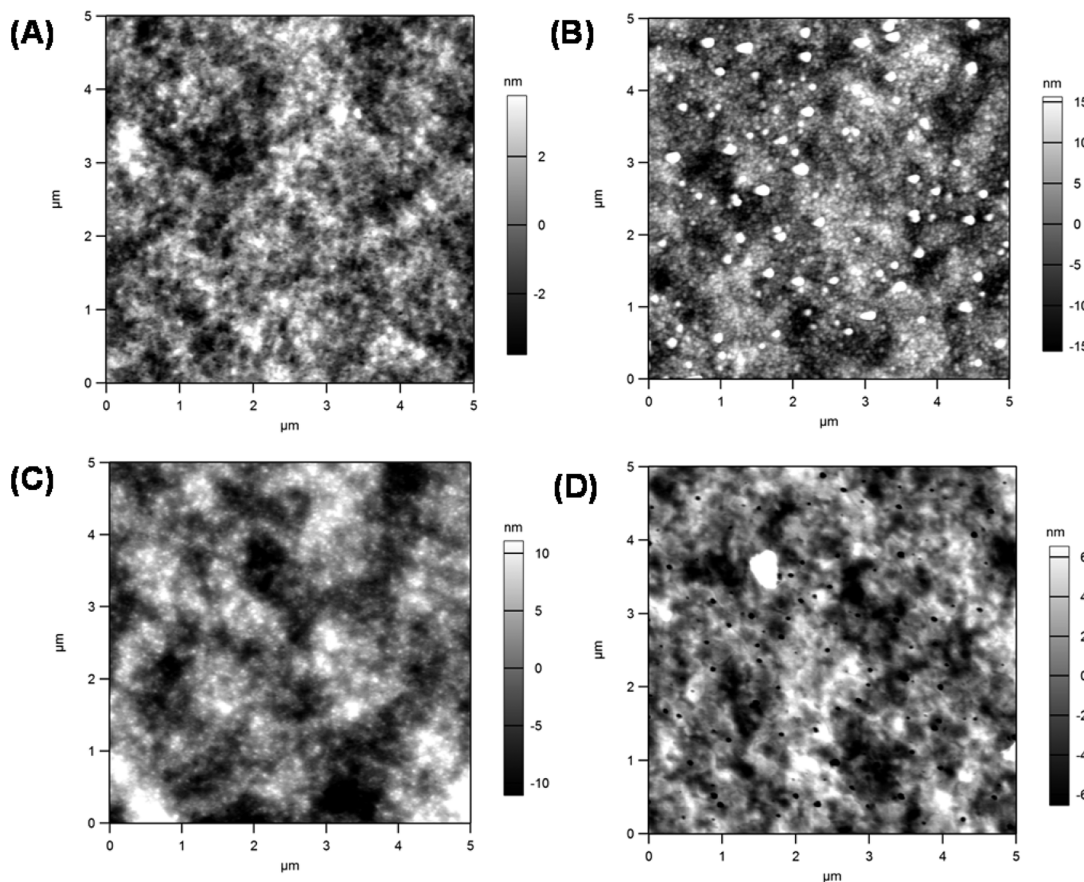


**Figure 5.** AFM topographical height images of the BHJ active layers of (A) PBnDT-FTAZ, (B) PSBnDT-FTAZ, (C) PBnDT-SeFTAZ, and (D) PSBnDT-SeFTAZ.

treatment via methanol<sup>43</sup>) which also help improving the device efficiency via various mechanisms. Since this work focuses on how the FTAZ system responds to structural modification, these device optimization methods will be further explored in future studies.

## CONCLUSIONS

Through this comparative study, it becomes clear that further improving the efficiency of existing high-performing donor polymers via structural modification is not straightforward. One can certainly manipulate the energy levels and band gaps by molecularly engineering the aromatic units within the conjugated backbone based on existing semiempirical methods.<sup>18</sup> For example, our results presented here show that selenophene incorporation and alkylthio substitution can tune the electro-optical properties of the original FTAZ polymer system. However, whether such changes (structural and related electro-optical) can translate into efficiency enhancement in the related BHJ devices is not easily predictable. In our study, replacing thiophene with selenophene successfully lowered the band gap and increased the  $J_{sc}$  of the devices, but overall efficiencies were mitigated by a lowered  $FF$ . On the other hand, the two alkylthio-substituted FTAZ polymers exhibited similar  $V_{oc}$  values in their BHJ devices as their alkyl analogues but also significant decreases in  $J_{sc}$  and therefore much lower efficiencies. All these results highlight that structurally optimizing the already high-performing polymer BHJ systems is very complex; a small structural perturbation to the existing conjugated polymer, e.g., backbone, side chain, or substituents,

can indeed improve certain device characteristics ( $V_{oc}$ ,  $J_{sc}$ , or  $FF$ ), but other desirable properties may be impaired.

While the photovoltaic results in this initial study do not exceed the original PBnDT-FTAZ's performance, the aim of this work was to establish how the FTAZ system would respond to these structural perturbations. Each new FTAZ polymer derivative exhibited moderate efficiencies (1.9–5.7%) with thick films (over 300 nm) and without additives or other efficiency-enhancing treatments, thereby demonstrating the promise of these structural modifications to this polymer system. Future work will explore processing conditions tailored specifically to alkylthio-substituted and selenophene-incorporated FTAZ polymers, focusing on overcoming low  $FF$  in selenophene-based polymers and low  $J_{sc}$  in alkylthio-substituted polymers to achieve optimum device performance.

## EXPERIMENTAL SECTION

**Reagents.** All monomers were synthesized according to the literature<sup>9,20</sup> with the exception of compound 3. All solvents are ACS grade unless otherwise noted. Tetrahydrofuran (THF) was dried by distillation from sodium/benzophenone. All other chemicals were purchased from commercial sources (Acros, Alfa Aesar, Sigma-Aldrich, Oakwood Chemical, Matrix Scientific) and used without further purification.

**4,8-Bis((2-butyoctyl)thio)benzo[1,2-*b*:4,5-*b'*]dithiophene (3).** To a solution of compound 1 (1.00 mmol, 0.396 g) dissolved in dry THF (50 mL) under an argon atmosphere, lithium aluminum hydride (4.00 mmol, 0.152 g) was added at 0 °C. The reaction mixture was then stirred for 2 h at room temperature. Afterward, the reaction was cooled down to 0 °C again, and 12-crown-4 ether (4.00 mmol, 0.65 mL) was added. The reaction mixture was stirred for another 1.5

h at 0 °C before adding 1-bromo-2-butyloctane (3.00 mmol, 0.758 g). The reaction mixture was then warmed to room temperature and stirred overnight. Afterward, the reaction was washed with saturated sodium bicarbonate and ethyl acetate. The organic layers were collected and dried over magnesium sulfate. The product was then purified by column chromatography using 5% methylene chloride/95% hexanes as the eluent. Yield: 65%. <sup>1</sup>H NMR (CDCl<sub>3</sub>, 400 MHz, δ): 7.76 (d, J = 5.2 Hz, 2H), 7.57 (d, J = 5.6 Hz, 2H), 3.01 (d, J = 5.6 Hz, 4H), 1.39 (m, 18H), 0.87 (m, 6H). <sup>13</sup>C NMR (CDCl<sub>3</sub>, 400 MHz, δ): 144.70, 140.40, 128.25, 123.92, 123.65, 40.46, 40.45, 38.47, 38.46, 33.03, 32.75, 31.82, 29.53, 28.74, 26.48, 22.92, 22.65.

**Instrumentation.** <sup>1</sup>H nuclear magnetic resonance (NMR) spectra were obtained at 400 MHz as solutions in CDCl<sub>3</sub>. <sup>13</sup>C NMR spectra were obtained at 100 MHz as solutions in CDCl<sub>3</sub> and C<sub>2</sub>Cl<sub>4</sub>D<sub>2</sub>. Chemical shifts are reported in parts per million (ppm, δ) and referenced from trimethylsilane. Coupling constants J are reported in hertz. Spectral splitting patterns are designated as s (singlet), d (doublet), dd (doublet of doublets), and m (multiplet). Gel permeation chromatography (GPC) measurements were carried out on a Polymer Laboratories PL-GPC 220 instrument using 1,2,4-trichlorobenzene as the eluent (stabilized with 125 ppm BHT) at 135 °C. The molecular weight is approximated relative to polystyrene standards. UV-vis absorption spectra were taken by a Shimadzu UV-2401PC spectrophotometer. For the measurement of thin films, polymers were spun-coat onto precleaned glass slides from ~10 mg/mL polymer solutions in chlorobenzene. Cyclic voltammetry measurements were performed on a Bioanalytical Systems (BAS) Epsilon potentiostat equipped with a three-electrode configuration: a glassy carbon working electrode, a Ag/AgNO<sub>3</sub> (0.01 M in anhydrous acetonitrile) reference electrode, and a Pt wire counter electrode. Measurements were taken under an argon atmosphere at a scan rate of 100 mV/s in anhydrous acetonitrile with tetrabutylammonium hexafluorophosphate (0.1 M) as the supporting electrolyte. Polymer films were drop-cast onto the glassy carbon electrode from a concentrated polymer solution in chloroform and dried under a stream of argon prior to obtaining measurements. The potential of the Ag/AgNO<sub>3</sub> reference electrode was internally calibrated by using the ferrocene/ferrocenium redox couple (Fc/Fc<sup>+</sup>). The electrochemical onsets were determined at the position where the current starts to deviate from the baseline. The highest occupied molecular orbital (HOMO) and lowest unoccupied molecular orbital (LUMO) energy levels were calculated from the onset oxidation potential (E<sub>ox</sub>) and onset reductive potential (E<sub>red</sub>), respectively, according to the following equations:

$$\text{HOMO} = -(E_{\text{ox}} + 4.8) \text{ (eV)}$$

$$\text{LUMO} = -(E_{\text{red}} + 4.8) \text{ (eV)}$$

**Polymer Solar Cell Fabrication and Testing.** Glass substrates coated with patterned tin-doped indium oxide (ITO) were purchased from Thin Film Devices, Inc. Prior to use, the substrates were cleaned via ultrasonication in deionized water, acetone, and then 2-propanol for 15 min each. The substrates were dried under a stream of nitrogen and then treated with UV-ozone for 15 min. A dispersion of poly(3,4-ethylene-dioxythiophene):poly(styrenesulfonic acid) (PEDOT:PSS) in water (Clevios PH500), filtered by a 0.45 μm poly(vinylidene fluoride) filter, was then spun-cast onto cleaned ITO substrates at 4000 rpm for 60 s and then baked at 130 °C for 15 min to give a thin film with a thickness of 40 nm. Blends of polymer and PC<sub>61</sub>BM (1:2 w/w, 12 mg/mL for polymers) were dissolved in corresponding solvents with heating at 120 °C for 6 h. All the solutions were filtered through a 5.0 μm poly(tetrafluoroethylene) (PTFE) filter and spun-cast at an optimized rpm for 60 s onto the PEDOT:PSS layer. The substrates were then dried at room temperature under vacuum for 30 min. The devices were finished for measurement after thermal deposition of a 30 nm film of calcium and a 100 nm film of aluminum as the cathode at a pressure of ~2 × 10<sup>-6</sup> mbar. There are 8 devices per substrate, with an active area of 12 mm<sup>2</sup> per device. The thicknesses of films were recorded by a profilometer (Alpha-Step 200, Tencor Instruments), and AFM Images were taken using an Asylum

Research MFP3D atomic force microscope. Device characterization was carried out under AM 1.5G irradiation with the intensity of 100 mW/cm<sup>2</sup> (Oriel 91160, 300 W) calibrated by a NREL certified standard silicon cell. Current densities versus potential (J-V) curves were recorded with a Keithley 2400 digital source meter. EQE were detected under monochromatic illumination (OrielCornerstone 260 1/4 m monochromator equipped with Oriel 70613NS QTH lamp), and the calibration of the incident light was performed with a monocrystalline silicon diode. All fabrication steps after adding the PEDOT:PSS layer onto ITO substrate, and characterizations were performed in gloveboxes under a nitrogen atmosphere.

For mobility measurements, the hole-only devices in a configuration of ITO/PEDOT:PSS (40 nm)/copolymer-PC<sub>61</sub>BM/Pd (50 nm) were fabricated. The experimental dark current densities J of polymer:PCBM blends were measured when applied with voltage from 0 to 4 V. The applied voltage V was corrected from the built-in voltage V<sub>bi</sub> which was taken as a compensation voltage V<sub>bi</sub> = V<sub>oc</sub> + 0.05 V and the voltage drop V<sub>rs</sub> across the ITO/PEDOT:PSS series resistance and contact resistance, which is found to be around 35 Ω from a reference device without the polymer layer. From the plots of L<sup>1.5</sup>J<sup>0.5</sup> vs V, hole mobilities of copolymers can be deduced from the equation

$$J = \frac{9}{8} \epsilon_r \epsilon_0 \mu_h \frac{V^2}{L^3}$$

where ε<sub>0</sub> is the permittivity of free space, ε<sub>r</sub> is the dielectric constant of the polymer which is assumed to be around 3 for the conjugated polymers, μ<sub>h</sub> is the hole mobility, V is the voltage drop across the device, and L is the film thickness of active layer.

## ASSOCIATED CONTENT

### Supporting Information

Synthetic procedures, NMR spectra for relevant intermediates and polymers, the photovoltaic performance of PBnDT-SeFTAZ with DIO additive, the SCLC hole mobility measurements, the picture of all polymers in chlorobenzene solutions, and cyclic voltammograms. This material is available free of charge via the Internet at <http://pubs.acs.org>.

## AUTHOR INFORMATION

### Corresponding Author

\*E-mail: wyou@unc.edu (W.Y.).

### Notes

The authors declare no competing financial interest.

## ACKNOWLEDGMENTS

This work was generously supported by the Office of Naval Research (Grant N000141110235) and the National Science Foundation (the CAREER Award DMR-0954280, the SOLAR Award DMR-1125803, and CHE-1058626). We also acknowledge Professor Richard F. Jordan and Mr. Ge Feng of the University of Chicago for GPC measurements.

## REFERENCES

- (1) Uy, R. L.; Price, S. C.; You, W. *Macromol. Rapid Commun.* **2012**, 33, 1162.
- (2) Yang, L.; Yan, L.; You, W. *J. Phys. Chem. Lett.* **2013**, 4, 1802.
- (3) Adebanjo, O.; Maharjan, P. P.; Adhikary, P.; Wang, M.; Yang, S.; Qiao, Q. *Energy Environ. Sci.* **2013**, 6, 3150.
- (4) Rao, A.; Chow, P. C. Y.; Gelinas, S.; Schlenker, C. W.; Li, C.-Z.; Yip, H.-L.; Jen, A. K.-Y.; Ginger, D. S.; Friend, R. H. *Nature* **2013**, 500, 435.
- (5) Tautz, R.; Da Como, E.; Limmer, T.; Feldmann, J.; Egelhaaf, H.-J.; von Hauff, E.; Lemaur, V.; Beljonne, D.; Yilmaz, S.; Dumsch, I.; Allard, S.; Scherf, U. *Nat. Commun.* **2012**, 3, 970.
- (6) Vandewal, K.; Albrecht, S.; Hoke, E. T.; Graham, K. R.; Widmer, J.; Douglas, J. D.; Schubert, M.; Mateker, W. R.; Bloking, J. T.;

- Burkhard, G. F.; Sellinger, A.; Fréchet, J. M. J.; Amassian, A.; Riede, M. K.; McGehee, M. D.; Neher, D.; Salleo, A. *Nat. Mater.* **2014**, *13*, 63.
- (7) Zhou, H.; Yang, L.; Stuart, A. C.; Price, S. C.; Liu, S.; You, W. *Angew. Chem., Int. Ed.* **2011**, *50*, 2995.
- (8) Sun, Y.; Takacs, C. J.; Cowan, S. R.; Seo, J. H.; Gong, X.; Roy, A.; Heeger, A. J. *Adv. Mater.* **2011**, *23*, 2226.
- (9) Price, S. C.; Stuart, A. C.; Yang, L.; Zhou, H.; You, W. *J. Am. Chem. Soc.* **2011**, *133*, 4625.
- (10) Su, M.-S.; Kuo, C.-Y.; Yuan, M.-C.; Jeng, U. S.; Su, C.-J.; Wei, K.-H. *Adv. Mater.* **2011**, *23*, 3315.
- (11) Huo, L.; Zhang, S.; Guo, X.; Xu, F.; Li, Y.; Hou, J. *Angew. Chem., Int. Ed.* **2011**, *50*, 9697.
- (12) Liang, Y.; Xu, Z.; Xia, J.; Tsai, S.-T.; Wu, Y.; Li, G.; Ray, C.; Yu, L. *Adv. Mater.* **2010**, *22*, E135.
- (13) Amb, C. M.; Chen, S.; Graham, K. R.; Subbiah, J.; Small, C. E.; So, F.; Reynolds, J. R. *J. Am. Chem. Soc.* **2011**, *133*, 10062.
- (14) Small, C. E.; Chen, S.; Subbiah, J.; Amb, C. M.; Tsang, S.-W.; Lai, T.-H.; Reynolds, J. R.; So, F. *Nat. Photonics* **2012**, *6*, 115.
- (15) Chu, T.-Y.; Lu, J.; Beaupré, S.; Zhang, Y.; Pouliot, J.-R.; Wakim, S.; Zhou, J.; Leclerc, M.; Li, Z.; Ding, J.; Tao, Y. *J. Am. Chem. Soc.* **2011**, *133*, 4250.
- (16) Park, S. H.; Roy, A.; Beaupre, S.; Cho, S.; Coates, N.; Moon, J. S.; Moses, D.; Leclerc, M.; Lee, K.; Heeger, A. J. *Nat. Photonics* **2009**, *3*, 297.
- (17) Zhou, H.; Yang, L.; Stoneking, S.; You, W. *ACS Appl. Mater. Interfaces* **2010**, *2*, 1377.
- (18) Zhou, H.; Yang, L.; You, W. *Macromolecules* **2012**, *45*, 607.
- (19) Tumbleston, J. R.; Stuart, A. C.; Gann, E.; You, W.; Ade, H. *Adv. Funct. Mater.* **2013**, *23*, 3463.
- (20) Lee, D.; Stone, S. W.; Ferraris, J. P. *Chem. Commun.* **2011**, *47*, 10987.
- (21) Lee, D.; Hubjari, E.; Kalaw, G. J. D.; Ferraris, J. P. *Chem. Mater.* **2012**, *24*, 2534.
- (22) Sista, P.; Biewer, M. C.; Stefan, M. C. *Macromol. Rapid Commun.* **2012**, *33*, 9.
- (23) Li, K.; Li, Z.; Feng, K.; Xu, X.; Wang, L.; Peng, Q. *J. Am. Chem. Soc.* **2013**, *135*, 13549.
- (24) Zhou, H.; Yang, L.; Price, S. C.; Knight, K. J.; You, W. *Angew. Chem., Int. Ed.* **2010**, *49*, 7992.
- (25) Uy, R.; Yang, L.; Zhou, H.; Price, S. C.; You, W. *Macromolecules* **2011**, *44*, 9146.
- (26) Zhou, E.; Cong, J.; Hashimoto, K.; Tajima, K. *Macromolecules* **2013**, *46*, 763.
- (27) Li, Y.; Pan, Z.; Miao, L.; Xing, Y.; Li, C.; Chen, Y. *Polym. Chem.* **2014**, *5*, 330.
- (28) Chen, H.-Y.; Yeh, S.-C.; Chen, C.-T.; Chen, C.-T. *J. Mater. Chem.* **2012**, *22*, 21549.
- (29) Alghamdi, A. A. B.; Watters, D. C.; Yi, H.; Al-Faifi, S.; Almeataq, M. S.; Coles, D.; Kingsley, J.; Lidzey, D. G.; Iraqi, A. *J. Mater. Chem. A* **2013**, *1*, 5165.
- (30) Kim, B.; Yeom, H. R.; Yun, M. H.; Kim, J. Y.; Yang, C. *Macromolecules* **2012**, *45*, 8658.
- (31) Shin, S. A.; Park, J. B.; Kim, J.-H.; Hwang, D.-H. *Synth. Met.* **2013**, *172*, 54.
- (32) Dou, L.; Chang, W.-H.; Gao, J.; Chen, C.-C.; You, J.; Yang, Y. *Adv. Mater.* **2013**, *25*, 825.
- (33) Kang, I.; An, T. K.; Hong, J.-a.; Yun, H.-J.; Kim, R.; Chung, D. S.; Park, C. E.; Kim, Y.-H.; Kwon, S.-K. *Adv. Mater.* **2013**, *25*, 524.
- (34) Lee, J.; Han, A. R.; Kim, J.; Kim, Y.; Oh, J. H.; Yang, C. *J. Am. Chem. Soc.* **2012**, *134*, 20713.
- (35) Lu, S.; Drees, M.; Yao, Y.; Boudinet, D.; Yan, H.; Pan, H.; Wang, J.; Li, Y.; Usta, H.; Facchetti, A. *Macromolecules* **2013**, *46*, 3895.
- (36) Saadeh, H. A.; Lu, L.; He, F.; Bullock, J. E.; Wang, W.; Carsten, B.; Yu, L. *ACS Macro Lett.* **2012**, *1*, 361.
- (37) Icli-Ozkut, M.; Ipek, H.; Karabay, B.; Cihaner, A.; Onal, A. M. *Polym. Chem.* **2013**, *4*, 2457.
- (38) Liu, Y.; Yang, Y.; Chen, C.-C.; Chen, Q.; Dou, L.; Hong, Z.; Li, G. *Adv. Mater.* **2013**, *25*, 4657.
- (39) Ballantyne, A. M.; Chen, L.; Nelson, J.; Bradley, D. D. C.; Astuti, Y.; Maurano, A.; Shuttle, C. G.; Durrant, J. R.; Heeney, M.; Duffy, W.; McCulloch, I. *Adv. Mater.* **2007**, *19*, 4544.
- (40) Thompson, B. C.; Fréchet, J. M. J. *Angew. Chem., Int. Ed.* **2008**, *47*, 58.
- (41) Roncali, J. *Macromol. Rapid Commun.* **2007**, *28*, 1761.
- (42) Heeney, M.; Zhang, W.; Crouch, D. J.; Chabinyc, M. L.; Gordelyev, S.; Hamilton, R.; Higgins, S. J.; McCulloch, I.; Skabara, P. J.; Sparrowe, D.; Tierney, S. *Chem. Commun.* **2007**, *5061*.
- (43) Zhou, H.; Zhang, Y.; Seifert, J.; Collins, S. D.; Luo, C.; Bazan, G. C.; Nguyen, T.-Q.; Heeger, A. J. *Adv. Mater.* **2013**, *25*, 1646.